A New Spectrophotometer System for Measuring Hemispherical Reflectance and Normal Emittance of Real Surfaces Simultaneously

Toshiro Makino and Hidenobu Wakabayashi

Department of Mechanical Engineering and Science, Kyoto University, Kyoto 606-8501, Japan.

A new spectrophotometer system is developed for the study of thermal radiation characteristics of real surfaces in thermal engineering environments. The system measures spectra of normal incidence hemispherical reflectance R_{NH} and normal emittance ε_N in the near-ultraviolet through infrared region of wavelength of 0.30 μm to 11 μm simultaneously and repeatedly with a cycle time of 4 s. The system enables evaluation of the normal incidence absorptance A_N in this wide spectral region. Spectrum transitions of specular-finished and rough-finished nickel surfaces in a high-temperature air-oxidation process are measured to demonstrate the performance of the system. Clear interference behaviors are found even in the spectra of hemispherical reflectance R_{NH} and emittance ε_N of a rough-finished surface.

Key Words : Hemispherical reflectance, Normal emittance, Real surface, Simultaneous measurement, Spectroscopic measurement, Thermal radiation

Nomenclature

A_N	normal incidence absorptance
n	index of refraction
R_{HH}	hemispherical reflectance for hemispherically homogeneous incidence
R_{HN}	normal reflectance for hemispherically homogeneous incidence
R_{NH}	normal incidence hemispherical reflectance
R_{NN}	normal incidence specular reflectance (specular reflection component of hemispherical reflectance R_{NH})
t	time after the start of heating specimen, s
T	temperature of specimen surface, K
ε_N	normal emittance
λ	wavelength of radiation in vacuum, m
σ	root-mean-square roughness, m

Subscripts

H	hemispherically homogeneous incidence, hemispherical reflection
N	normal (15^o-direction in measurement) incidence, reflection, and emission

1 Introduction

In the thermal engineering study of thermal radiation characteristics of solids, spectroscopic experiments on real surfaces are important. Real surfaces have a variety of microstructures, and they change with time. Radiation characteristics of the surfaces change sensitively with changes of the microstructure. Such characteristics should be investigated in a wide spectral region of near-ultraviolet through infrared for thermal engineering applications.

The authors have developed a wide-spectral-region high-speed spectrophotometer system [1]. This system measures spectra of normal incidence specular reflectance R_{NN} and normal emittance ε_N in a spectral region of wavelength of 0.30 μm to 11 μm simultaneously and repeatedly at every 2 s. On the basis of this hardware system, the authors clarified the dynamics of radiation phenomena of real surfaces [2], and developed a real-time measurement technique for diagnosing the temperature and microstructure of real surfaces [3]. They also suggested the possibility of developing a spectrally-functional emitter surface for thermophotovoltaic (TPV) electric power generation [4]. From the above investigations, they have suggested a method for studies on thermal radiation characteristics of real surfaces in the field of thermal engineering [5].

However, an effective technique has not been developed for measuring spectra of absorptance of real surfaces. It means that a numerous number of absorption spectra in arbitrary units have been measured for qualitative analyses of the chemical composition of materials, but that we need spectra of absorptance for quantitative evaluation of radiation energy absorption of real surfaces whose surface microstates change in thermal engineering environments. A new idea and experimental setup should be developed to measure the transition of the absorptance of real surfaces for thermal engineering applications.

In the present study, we develop a new spectrophotometer system on the basis of the above-mentioned system [1] to measure the spectra of normal incidence hemispherical reflectance R_{NH} and normal emittance ε_N in the spectral region of wavelength of 0.30 μm to 11 μm simultaneously and repeatedly at every 4 s. Most real surfaces of thermal engineering are diffusely reflecting and diffusely emitting. This spectrophotometer system measures the spectra of reflectance R_{NH} and emittance ε_N of such real surfaces accurately to satisfy the definitions of the reflectance and emittance.

Thus, as far as non-transparent surfaces, spectra of normal incidence absorptance A_N are evaluated from the spectra of reflectance R_{NH} in this wide spectral region. We present an idea of the spectrophotometer system, describe the details of a new incident optics sub-system of the spectrophotometer system, and demonstrate the performance of the system by two series of spectral measurements on real surfaces which are changing the microstructure in a high-temperature environment.

2 Idea for New Spectrophotometer System

Kirchhoff's law on thermal radiation holds between the (spectral) emittance and (spectral) absorptance, and the normal emittance ε_N is equal to the normal incidence absorptance A_N,

$$\varepsilon_N = A_N \tag{1}$$

This relation should be verified experimentally in principle [6]. Even when this relation is verified, the measurement of a spectrum of either emittance ε_N or absorptance A_N is not sufficient for thermal engineering applications.

The measurement of a spectrum of emittance is not particularly easy on a surface at a not-so-high temperature and in a shorter wavelength region. The measurement is also not easy on a non-metallic surface. These difficulties are due to the following reasons: (i) The measurement of radiation energy is not easy in a spectral region of low (λT) values, where λ is the wavelength of radiation in vacuum and T is the temperature of the surface, because the spectral intensity of radiation is not sufficient for accurate detection in such a region. (ii) The measurement of the surface temperature is not easy on a non-metallic surface on which a thermocouple cannot be welded, and the emittance cannot be determined well. And, (iii) a problem is emphasized on the measurement on a surface whose absorption of radiation is not strong and the radiation

emitted in the inner parts of the material emanates out of the surface. Such materials of the surfaces are mostly low in thermal conductivity and they have a temperature distribution in the depth direction in the emittance measurement setup, where the specimen is heated from the back. In this case volumetric emission of radiation from the inner parts of the material with a temperature distribution is measured, and the definition of emittance is not clear.

On the other hand, the measurement of absorptance spectra is not easy on real surfaces of thermal engineering interests. For non-transparent solid materials, the spectral measurement of absorptance is substituted by the measurement of reflectance. Since such surfaces reflect radiation more or less anisotropically and diffusely, radiation energy reflected over the hemisphere should be measured to determine the hemispherical reflectance.

For non-transparent surfaces an energy conservation law holds between the absorptance A_N and reflectance R_{NH},

$$R_{NH}+A_N=1 \tag{2}$$

From Eqs. 1 and 2 the following relation is drawn:

$$\varepsilon_N = A_N =1- R_{NH} \tag{3}$$

The spectrum of absorptance A_N is obtained by the measurement of a spectrum of reflectance R_{NH} and the complementary relation (Eq. 2), and the spectrum of emittance ε_N is obtained by the assumption of Kirchhoff's law (Eq. 1). The temperature measurement is not so essential in the reflectance measurement as in the emittance measurement. Thus, the above-mentioned problems (i) to (iii) are overcome, if a spectrum of hemispherical reflectance R_{NH} can be measured properly.

The hemispherical reflectance has been measured by various techniques [7-13]. In the field of thermal engineering, the hemispherical reflectance has been measured mainly by an integrating sphere technique [7]. Integrating sphere attachments for

spectrophotometers are commercially available. But the reflectance measured by this technique is not a rigorously defined hemispherical reflectance. The reflectance does not distinguish rigorously between the normal incidence hemispherical reflectance R_{NH} and the hemispherical reflectance R_{HH} for hemispherically homogeneous incidence. The reflectance R_{NH} and reflectance R_{HH} can be different from each other by as much as 10 % in absolute value [14]. A new measurement technique for the reflectance R_{NH} should be developed.

For the design of a new spectral measurement setup, consideration for the arrangement of an incident optics sub-system and spectrometer sub-system is important. For the spectrophotometer system in which white radiation is incident on the specimen surface and reflected radiation is optically dispersed and detected, the direct measurement of the normal incidence hemispherical reflectance R_{NH} is not easy on the basis of radiation energy measurement. In this case the normal reflectance R_{HN} for hemispherically homogeneous incidence on the radiation intensity is better to be measured. Here, the Helmholtz reciprocity principle holds between the reflectance R_{NH} and reflectance R_{HN} [15],

$$R_{NH}=R_{HN} \tag{4}$$

Thus, by measuring a spectrum of reflectance R_{HN} and by applying Eqs. 3 and 4, spectra of absorptance A_N and emittance ε_N are evaluated. The present study adopts this procedure.

3 Incident Optics Sub-System of New Spectrophotometer System

Figure 1a shows a sketch of the newly designed incident optics sub-system for the simultaneous measurement of spectra of reflectance R_{HN} and emittance ε_N. Figure 1b shows a photograph of the sub-system, where specimen /5/ is substituted by a

blackbody for emittance calibration. Figure 2 shows a schematic diagram of the new wide-spectral-region high-speed spectrophotometer using the incident optics sub-system shown in Fig. 1a.

Figures 1(a), 1(b), 2

In Fig. 1a two paraboloidal mirrors /3/ and /4/ of 120 mm in diameter are set facing each other. The two paraboloidal mirrors have holes of 12 mm in diameter in the central parts. A tungsten-halogen lamp /1/ for the near-ultraviolet through near-infrared region or an Si_3N_4 light source /2/ for the infrared region is set at the focal point of the paraboloidal mirror /3/. The sizes of the light sources /1/ and /2/ are 3.3 mm × 0.6 mm and 4.7 mm × 1.3 mm, respectively. The two light sources are alternatively set at the focal point of the paraboloidal mirror /3/ or at an off-focal point by the help of cam mechanics /C/ (in Fig. 2) driven by a computer-controlled stepping motor.

The small light sources emit radiation whose intensity is approximately isotropic. When one of the two light sources is set at the focal point of the paraboloidal mirror /3/, the emitted radiation is transformed by the paraboloidal mirror to a parallel flux to proceed to another paraboloidal mirror /4/. A specimen /5/ is set at the focal point of the paraboloidal mirror /4/. On the surface of the specimen /5/, radiation whose intensity is hemispherically homogeneous is incident from the paraboloidal mirror /4/ and focuses. The specimen surface reflects radiation over the hemisphere. A portion of the reflected radiation which proceeds in the normal direction is led through a hole on the paraboloidal mirror /4/ to the spectrometer and detector sub-systems and measured. In addition, the specimen surface at high temperatures emits radiation over the hemisphere. A portion of the emitted radiation which proceeds in the normal direction is led through a hole on the paraboloidal mirror /4/ to the spectrometer and detector sub-systems and measured. Both the reflected radiation and emitted radiation are

measured at the same time in this case. On the other hand, when both light sources /1/ and /2/ are set at an off-focal point, radiation is not incident on the specimen surface and only the emitted radiation in the normal direction is measured. From these two kinds of measured values, the reflection and emission components are readily separated.

Measured reflection values are calibrated by the measured values on a reflectance standard surface. The reflectance standard surface is an optically smooth surface of nickel, whose reflectance is calculated on the basis of an optical constant spectrum [16]. Measured emission values are calibrated by the measured values on a blackbody. The blackbody is of a cylinder-type, 20 mm in inner diameter and 50 mm in depth, which has a diaphragm aperture of 10 mm in inner diameter. It is made of stainless steel SUS304 whose inner surface is sufficiently air-oxidized. The apparent normal emittance is estimated to be 0.99. The photograph of Fig. 1b shows this blackbody which is set at the position of specimen /5/ in the emittance calibration process.

In Fig. 2, /1/ to /6/ and /C/ compose the incident optics sub-system for the measurement of the reflectance R_{HN} and emittance ε_N, and /7/ to /20/ compose spectrometer and detector sub-systems of the spectrophotometer system. The system of Fig. 2 measures the spectra of reflectance R_{HN} and emittance ε_N at 93 wavelength points in a spectral region of 0.30 μm to 11 μm simultaneously and repeatedly with a cycle time of 4 s. But the spectral region of emittance measurement is restricted depending on the temperature of the specimen surface. The reflectance R_{HN} measured by this system is equal to the reflectance R_{NH}, as shown in Eq. 4.

In the actual measurement the specimen surface is set by being inclined as much as 15^o from the optical axis of the two paraboloidal mirrors /3/ and /4/ so that the specular reflection component in the hemispherical reflection can be accurately measured. That is, subscript N in reflectances R_{HN}, R_{NH}, and emittance ε_N corresponds actually to 15^o

in this measurement. The solid angle of the holes in the center of the paraboloidal mirrors is less than 0.12 sr. The solid angle excluding the measured hemispherical reflection by the 15° inclination of the specimen is less than 0.30 sr. Influence of the 15° inclination to the measured R_{HN} values is only 0.02 % at most. Random errors in the measured reflectance R_{NH} are evaluated to be the order of ±1 % and ±10 % at λ=0.70 μm and at 8.0 μm, respectively, in the relative value. Random errors in the measured emittance ε_N of the surface at 1100 K are evaluated to be the order of ±2 % and ±4 % at λ=3.5 μm and at 8.0 μm, respectively, in the relative value. For surfaces at temperatures lower than 1100 K, random errors in the measured emittance ε_N are larger. The uncertainty of R_{NH} and ε_N measurements in the infrared wavelength region is determined mostly by the instability of the infrared detector elements.

4 Spectrum Transition of Metal Surface in Oxidation Process

In order to demonstrate the performance of the developed spectrophotometer system, transitions of spectra of normal reflectance R_{HN} for hemispherically homogeneous incidence and normal emittance ε_N are measured on nickel surfaces in a high-temperature air-oxidation process. The materials of the specimens are a nickel plate of 99.95 % in purity and 1 mm in thickness. Two kinds of nickel surfaces are prepared: a specular-finished surface which is buffed to realize an optical smoothness with a maximum roughness less than 30 nm, and a rough-finished surface which is wet-ground on grinding powders of mesh JIS-#240. The root-mean-square roughness σ of the rough-finished surface is of the order of 2 μm. The two kinds of surfaces are heated in air at a heating rate of 1 $K \cdot s^{-1}$ up to 1100 K and kept at the temperature for 1 h. The surface temperature is measured by a K-thermocouple of 100 μm in diameter welded on the specimen surface. The developed spectrophotometer system is employed

to measure the spectra of reflectance R_{HN} at 93 wavelength points in a near-ultraviolet through infrared region of 0.30 μm to 11 μm and the spectra of emittance ε_N at 42 wavelength points in an infrared region of 2.0 μm to 11 μm simultaneously at every 4 s. In this experiment an oxide film is formed on the surface, and the film surface roughens with the inhomogeneous growth of the crystal grains of the film even on the specular-finished surface. In response to the sensitive changes in surface microstructure, the radiation spectra change drastically.

Figures 3-6 show the experimental results where the measured reflectance R_{HN} is shown as the reflectance R_{NH}. Figures 3 and 4 are for the specular-finished surface, and Figs. 5 and 6 are for the rough-finished surface. Figures 3 and 5 show the transitions of spectra of reflectance R_{NH} and emittance ε_N. The time t after the start of heating the specimen flows from back to forward in the figures. Figures 4 and 6 show the time transitions of reflectance R_{NH} and emittance ε_N at the wavelength points of the measurements. In Figs. 4 and 6 the reflectance R_{NH} and emittance ε_N are plotted on a logarithmic scale so that the absolute values can be read to the significant figure of unity. The reflectance R_{NH} curves, whose valleys of oscillation are located on the left side, are those at the shorter wavelengths, and the emittance ε_N curves, whose peaks of oscillation are located on the left side, are those at the shorter wavelengths.

Figures 3~6

In previous studies [1-5] transitions of the spectra of normal incidence specular reflectance R_{NN} and normal emittance ε_N were measured on a specular-finished surface in an air-oxidation process, and oscillations of the spectrum of film interference were observed clearly in the spectra of emittance ε_N as well as in the spectra of reflectance R_{NN}. In the present study spectra of normal incidence hemispherical reflectance R_{NH} and normal emittance ε_N are measured simultaneously for the first time, and it is found that spectra of hemispherical reflectance R_{NH} of the specular-finished surface in the

air-oxidation process have also the oscillations of interference, as seen in Figs. 3 and 4. It is also found that spectra of hemispherical reflectance R_{NH} and emittance ε_N of the rough-finished surface in the air-oxidation process have oscillations of interference, as seen in Figs. 5 and 6.

The specular-finished surface roughens in the surface oxidation process, but the roughness σ is of the order of 300 nm even at the last stage of the experiment. On the other hand, the rough-finished surface is already rough before the oxidation whose roughness σ is of the order of 2 μm. These values of roughness σ are measured by a laser optical microscope, whose nominal value of the minimum resolution is 10 nm. The interference in hemispherical reflectance R_{NH} of the rough-finished surface seems to be unexpected, but it can be explained as follows. In the micro-profile of the cross section of a rough surface, the inclination of elementary micro-surfaces is of the order of 15^o at most and the oxide film substantially grows as a parallel film by tracing the micro-profile of the substrate. The index of refraction n of the film is of the order of 2 in the spectral region of the present measurements, and the critical angle of inner reflection of radiation inside the film is of the order of 30^o. Thus, the incident angle dependence of the optical length for radiation traveling in the film is weak, and radiation interference appears even in the hemispherical reflection spectra of a rough-finished surface which is composed mostly of the diffuse reflection component. The absolute values of the reflectance R_{NH} of the rough-finished surface are lower than those of the specular-finished surface. It should be noted that the ordinates of Figs. 5 and 6 are magnified by a factor of two compared to those of Figs. 3 and 4.

In previous studies [1-5], the normal incidence specular reflectance R_{NN} of a specular-finished metal surface decreased siginificantly in the air-oxidation process, particularly in the shorter wavelength region. The authors of the studies have explained that this phenomenon is caused mainly by the increase of the diffraction or scattering

of radiation on the roughened surface. But by considering the values of the hemispherical reflectance R_{NH} in the shorter wavelength region in Figs. 3-6 and by considering the energy conservation law (Eq. 2), it is clarified that the decrease of the reflectances R_{NN} and R_{NH} is caused by the increase of absorption of radiation by the oxide film on the surface.

Using the present spectrophotometer system to measure the reflectance R_{NH} and emittance ε_N simultaneously on various surfaces of the same surface microstates, the complementary relation $R_{NH}+\varepsilon_N=1$ between reflectance R_{NH} and emittance ε_N shown in Eq. 3, which was driven for a thermal equilibrium system, can be examined for non-equilibrium systems in the present experiment. The relation, which is derived from Kirchhoff's law on thermal radiation, should be examined more extensively for other non-equilibrium systems in thermal engineering [6]. By comparing Figs. 3-6 qualitatively, it is found that the wavelength λ and time t of the valleys of the oscillations of interference of reflectance R_{NH} and those of the peaks of the oscillations of interference of emittance ε_N agree well with each other.

From the above experiment the newly developed spectrophotometer system is demonstrated to be effective to measure the spectra of reflectance R_{NH} and emittance ε_N of real surfaces whose surface microstructure changes with time and the reflection is more or less diffuse. Particularly on non-transparent surfaces, the normal incidence absorptance A_N (=1-R_{NH}) or normal emittance ε_N can be measured in the wide spectral region of 0.30 μm to 11 μm and in the wavelength and temperature region of low (λT) values where measurements of a spectrum of emittance ε_N are not easy.

5 Conclusions

In the present study we have developed a new spectrophotometer system for

measuring thermal radiation characteristics of real surfaces in thermal engineering environments. Concluding remarks are summarized as follows:

(1) Spectra of normal incidence hemispherical reflectance R_{NH} and normal emittance ε_N have been measured in a near-ultraviolet through infrared region of 0.30 μm to 11 μm simultaneously and repeatedly at every 4 s.

(2) Spectra of normal incidence absorptance A_N have been evaluated on diffusely-reflecting surfaces and in a wide spectral region. By assuming Kirchhoff's law on thermal radiation, spectra of emittance ε_N can be evaluated even in the shorter wavelength region as that of the direct measurement of ε_N.

(3) It has been found that clear behavior of radiation interference appears even in the spectra of normal incidence hemispherical reflectance R_{NH} of an air-oxidized rough-finished metal surface.

Acknowledgments

This project has been supported by the Grant-in-Aid for Scientific Research ((A)20246039) of the Ministry of Education, Culture, Sports, Science and Technology, Japan. The authors have accepted invaluable assistance from the co-researchers of the project, Professors K. Hanamura, J. Yamada, K. Miyazaki, and M. Matsumoto.

References

1. H. Wakabayashi, T. Makino, Meas. Sci. Technol., **12**, 2113 (2001)
2. T. Makino, in *Heat Transfer 2002*, **1**, ed. by J. Taine, (Elsevier, Paris, 2002), pp.55-66
3. T. Makino, H. Wakabayashi, JSME Int. J., Ser.B, **46**, 500 (2003)

4. T. Makino, H. Wakabayashi, in ~~*Proceedings of the*~~ *13th International Heat Transfer Conference*, CD-ROM, (2006), No.RAD-11
5. T. Makino, in ~~*The*~~ *18th International Symposium on Transport Phenomena*, CD-ROM, (2007), ~~pp.136-145,~~ No.Keynote 116
6. T. Makino, H. Wakabayashi, in ~~*Proceedings of the 14th*~~ *International Heat Transfer Conference (IHTC14)*, CD-ROM, (2010), No.IHTC14-22718
7. D.K. Edwards, in *Measurements in Heat Transfer*, ed. by E.R.G. Eckert, R.J. Goldstein, (Hemisphere Pub., Washington, D.C., 1976), pp.425-473
8. N. Terada, K. Ohnishi, M. Kobayashi, T. Kunitomo, Int. J. Thermophys., **7**, 1101 (1986)
9. J.R. Markham, K. Kinsella, R.M. Carangelo, C.R. Brouillette, Rev. Sci. Instrum. **64**, 2515 (1993)
10. K.A. Snail, L.M. Hanssen, Appl. Optics, **37**, 4143 (1998)
11. A. Seifter, K. Boboridis, A.W. Obst, Int. J. Thermophys., **25**, 547 (2004)
12. L.M. Hanssen, C.P. Cagran, A.V. Prokhorov, S.N. Mekhobtsev, V.B. Khromchenko, Int. J. Thermophys., **28**, 566 (2007)
13. H.J. Lee, A.C. Bryson, Z.M. Zhang, Int. J. Thermophys., **28**, 918 (2007)
14. T. Makino, T. Yoshida, S. Tanaka, Heat Transfer - Japanese Res., **23**, 103 (1995)
15. R. Siegel, J.R. Howell, *Thermal Radiation Heat Transfer*, 3rd edn., (Taylor & Francis, Bristol , 1992), pp.47-91
16. T. Makino, H. Kawasaki, T. Kunitomo, Bull. JSME, **25**, 804 (1982)

Figure Captions

Fig. 1 (a) Sketch of incident optics sub-system for simultaneous measurement of spectra of reflectance R_{HN} and emittance ε_N and (b) photograph of incident optics sub-system, where specimen /5/ is substituted by a blackbody for emittance calibration

Fig. 2 Schematic diagram of wide-spectral-region high-speed spectrophotometer system for measuring reflectance R_{HN} and emittance ε_N

Fig. 3 Spectrum transition of reflectance R_{NH} and emittance ε_N of a specular-finished nickel surface in a high-temperature air-oxidation process

Fig. 4 Time transition of reflectance R_{NH} and emittance ε_N of a specular-finished nickel surface in a high-temperature air-oxidation process

Fig. 5 Spectrum transition of reflectance R_{NH} and emittance ε_N of a rough-finished nickel surface in a high-temperature air-oxidation process

Fig. 6 Time transition of reflectance R_{NH} and emittance ε_N of a rough-finished nickel surface in a high-temperature air-oxidation process

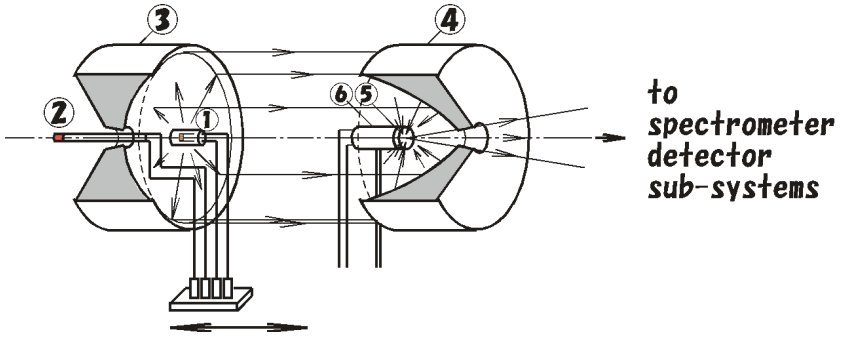

/1/ tungsten-halogen lamp
/2/ Si_3N_4 light source
/3/ paraboloidal mirror 1
/4/ paraboloidal mirror 2
/5/ specimen
/6/ heater

(a)

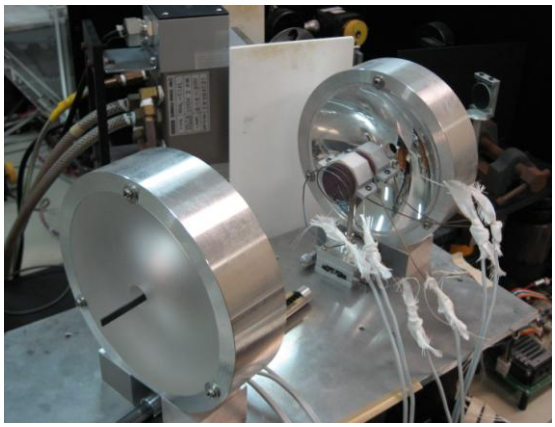

(b)

Fig. 1

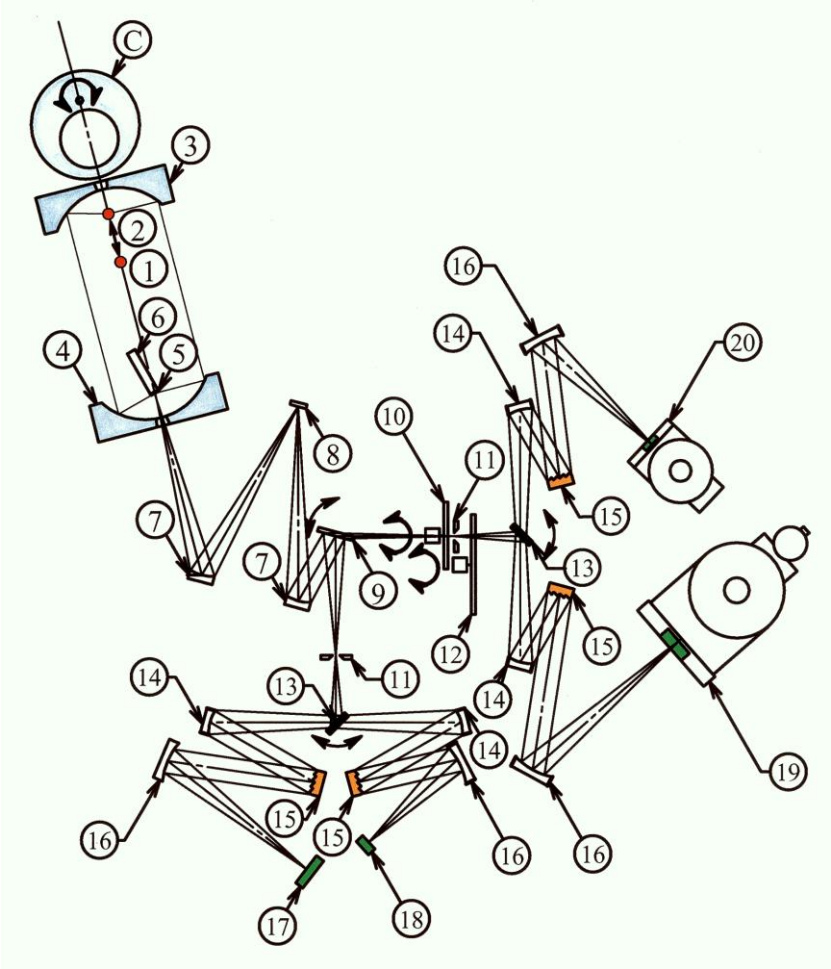

/1/ tungsten-halogen lamp
/2/ Si_3N_4 light source
/3/ paraboloidal mirror 1
/4/ paraboloidal mirror 2
/5/ specimen
/6/ heater
/7/ concave mirror
/8/ plane mirror
/9/ rotational plane mirror
/10/ chopper
/11/ entrance slit
/12/ filter disk
/13/ rotational plane mirror
/14/ collimator
/15/ diffraction grating
/16/ camera mirror
/17/ 35-Si photodiode array
/18/ 16-Ge photodiode array
/19/ 32-InSb photovoltaic detector array
/20/ 16-HgCdTe photoconductive detector array
/C/ cam mechanics

Fig. 2

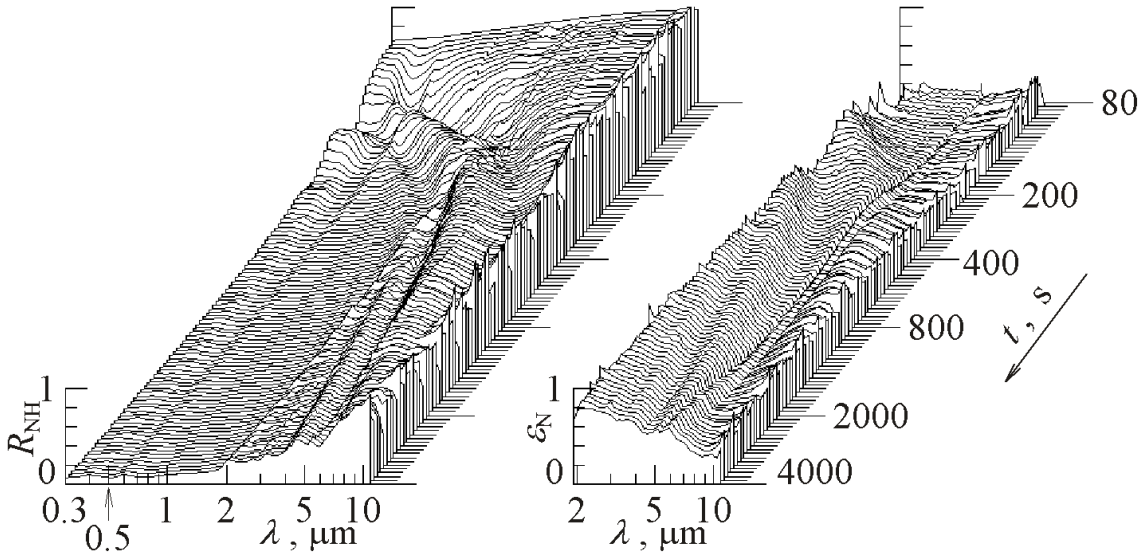
R_{NH}
1
0
0.3
0.5
1
2
5
10
λ, μm
ε_N
1
0
2
5
10
λ, μm
80
200
400
800
2000
4000
t, s

Fig. 3

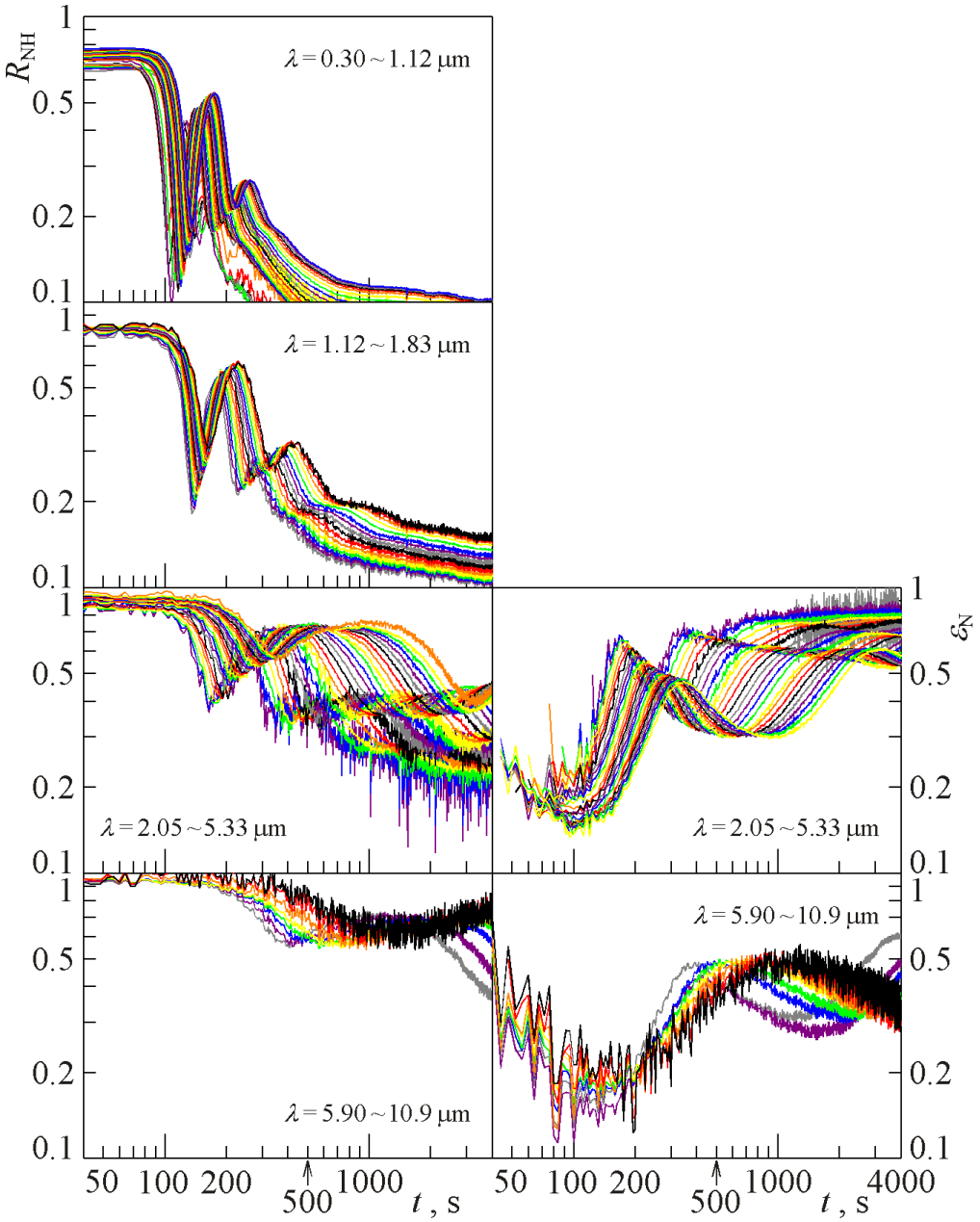
R_{NH}
ε_N
λ = 0.30 ~ 1.12 μm
λ = 1.12 ~ 1.83 μm
λ = 2.05 ~ 5.33 μm
λ = 2.05 ~ 5.33 μm
λ = 5.90 ~ 10.9 μm
λ = 5.90 ~ 10.9 μm
1
0.5
0.2
0.1
50 100 200 500 1000
50 100 200 500 1000 4000
t , s
t , s

Fig. 4

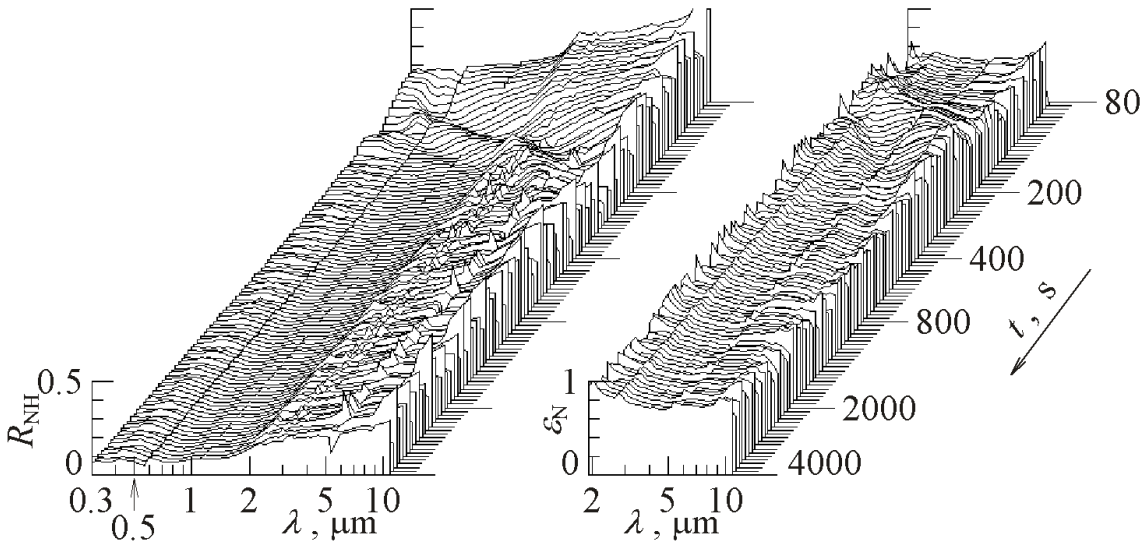
R_{NH}
0.5
0
0.3
0.5
1
2
5
10
λ, μm
ε_N
1
0
2
5
10
λ, μm
80
200
400
800
2000
4000
t, s

Fig. 5

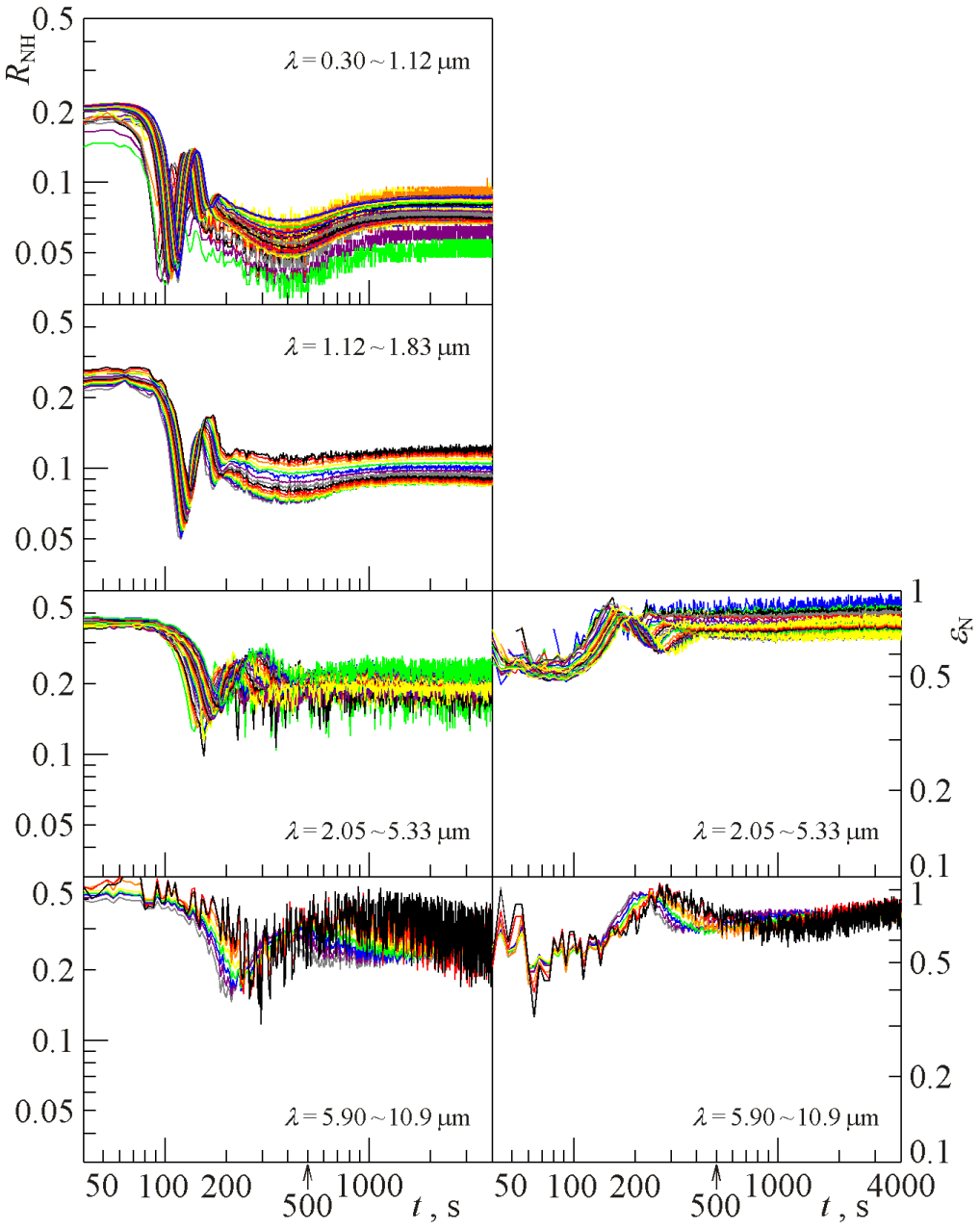
R_{NH}
ε_N
$\lambda = 0.30 \sim 1.12$ μm
$\lambda = 1.12 \sim 1.83$ μm
$\lambda = 2.05 \sim 5.33$ μm
$\lambda = 2.05 \sim 5.33$ μm
$\lambda = 5.90 \sim 10.9$ μm
$\lambda = 5.90 \sim 10.9$ μm
0.5
0.2
0.1
0.05
1
0.5
0.2
0.1
50 100 200 500 1000 t, s
50 100 200 500 1000 4000 t, s

Fig. 6